The Iron-Histidine Mode of Myoglobin Revisited: Resonance Raman Studies of Isotopically Labeled *Escherichia coli* Expressed Myoglobin

Andrew V. Wells,[†] J. Timothy Sage,[†] Dimitrios Morikis,[†,§] Paul M. Champion,*[,†] Mark L. Chiu,[‡] and Stephen G. Sligar[‡]

Contribution from the Department of Physics, Northeastern University, Boston, Massachusetts 02115, and Departments of Chemistry, Biochemistry, Physiology, and Biophysics, and The Beckman Institute for Advanced Science and Technology, University of Illinois at Urbana—Champaign, Urbana, Illinois 61801. *Received April 23, 1991*

Abstract: Resonance Raman spectra of *E. coli* expressed sperm whale metMb, deoxyMb, and MbCO, with ^{15}N-labeled globin nitrogens, are used to identify modes which are associated with the heme axial ligand His(F8). We have observed an isotopic shift of 1.25 cm^{-1} in the 218-cm^{-1} mode of deoxyMb, which suggests a Fe–His mode assignment as previous isotopic labeling studies have indicated. The magnitude of this shift agrees with the calculated shift for a two-body oscillator involving the Fe and imidazole His(F8) masses. However, additional isotopic labeling studies, involving $^{54}Fe/^{57}Fe$, $^{15}N_p/^{14}N_p$, and $^{2}H/^{1}H$ cannot be explained quantitatively within this model. As a result, we explore some simple variations on the two-body oscillator and find that a model involving concerted motion of the iron and N_ϵ of the histidine against the rest of the imidazole ring is more consistent with the entire body of experimental evidence. This model is overly simplistic, but suggests that contributions from internal modes of the His(F8) cannot be ignored. Earlier data on the site-directed Mb mutants His(F8)Tyr show that modes at ~250 cm^{-1} in metMb and MbCO (along with the 218 cm^{-1} of deoxyMb) disappear upon removal of the Fe–His bond, suggesting a ν_{Fe-His} assignment. However, the resonance Raman spectra of MbCO at pH 3.9, metHb, HbCO, and HbO_2 also lack the modes at ~250 cm^{-1} even though they are known to have intact Fe–His bonds. Furthermore, we do not observe any significant $^{15}N_{His}$ isotopic shifts in the modes at ~250 cm^{-1} or in any other modes of metMb and MbCO. Thus, the modes at ~250 cm^{-1} in metMb and MbCO cannot be assigned to any motion that involves the labeled His(F8) nitrogens. Instead, the data presented here suggests that the modes at ~250 cm^{-1} are structurally sensitive out-of-plane heme modes that are enhanced via interactions between the heme and His(F8). Moreover, there must be a subtle structural difference between the heme–His(F8) geometry of Mb and Hb that accounts for the Raman activity of the modes at ~250 cm^{-1} in metMb, MbCO, and MbO_2 at pH 7 and the absence of these modes in the analogous Hb complexes.

Introduction

Low-frequency resonance Raman modes of heme proteins have long been studied because of the possibility of detecting axial ligand modes by isotopic labeling.[1-4] Of particular interest is the identification of the stretching frequency of the covalent bond linking the heme group to the protein, which in the O_2 storage and transport proteins is the iron–histidine (Fe–His) mode. This mode has already been identified in deoxymyoglobin(deoxyMb)[2,5] and in deoxyhemoglobin(deoxyHb).[2,6,7] One objective of this work is to attempt to identify the corresponding Fe–His modes in metMb and MbCO by isotopic labeling of the globin nitrogens. Isotopic labeling of the heme iron atom has been studied previously in Mb and a 1.7-cm^{-1} isotopic shift of the 218-cm^{-1} mode was observed,[5] consistent with an Fe–His mode assignment. However, since out-of-plane heme modes might also be expected to show an isotopic shift with Fe labeling, there is potential ambiguity in the interpretation of shifts involving isotopically labeled Fe in heme proteins. Argade et al.[5] helped to resolve this ambiguity by observing no downshift in the 218-cm^{-1} mode in samples reconstituted with $^{15}N_p$-labeled heme, thus eliminating the possibility of an out-of-plane Fe–N_p assignment. The suggestion that the iron isotopic shift of the 218-cm^{-1} mode is due to an in-plane Fe–N_p vibration[8a] (N_p, porphyrin nitrogen) is not consistent with the (totally symmetric) polarization properties of this band.[8b] A more direct approach, employed here, takes advantage of recent advances in protein engineering[9] and utilizes samples produced by *Escherichia coli* with ^{15}N-labeled globin nitrogens (i.e., $^{15}N_{His}$) and reconstituted with unlabeled heme.

Isotopic shifts involving Fe have been observed in the 274-cm^{-1} band of ferric HRP and in the 246-cm^{-1} band of metMb, and these frequencies have been previously assigned to Fe–His stretching.[3] In addition, it has been observed that low-frequency modes in the ~250-cm^{-1} region of metMb and MbCO must be associated with the presence of His(F8) since they disappear when the His(F8) ligand is replaced.[10,11] However, the absence of any ~250-cm^{-1} modes in metHb, HbCO, and HbO_2 indicates that the appearance of the ~250-cm^{-1} mode depends on more than simple Fe–His ligation. Here, we discuss the globin isotopic labeling results, along with evidence from Mb His(F8)Tyr mutant studies[10,11] that give insight into the assignments of the modes at ~250 cm^{-1} in metMb, MbO_2, and MbCO.

Materials, Methods, and Data Analysis

The ^{15}N-labeled wild-type sperm whale myoglobin was grown on *E. coli* with [^{15}N]ammonium sulfate as the sole nitrogen source.[9] The level

* Author to whom correspondence should be addressed at Northeastern University.
† Northeastern University.
‡ University of Illinois.
§ Present address: Department of Molecular Biology, MB2, The Scripps Research Institute, La Jolla, CA 92037.

(1) Yu, N.-T.; Kerr, E. A. In *Biological Applications of Raman Spectroscopy*; Spiro, T. G., Ed.; Wiley: New York, 1988; Vol. 3, pp 39-95.
(2) Kitagawa, T.; Nagai, K.; Tsubaki, M. *FEBS Lett.* **1979**, *104*, 376-378.
(3) Teraoka, J.; Kitagawa, T. *J. Biol. Chem.* **1981**, *356*, 3969-3977.
(4) (a) Choi, S.; Spiro, T. G. *J. Am. Chem. Soc.* **1983**, *105*, 3683-3692. (b) Spiro, T. G. In *Iron Porphyrins*; Lever, A. B. P., Gray, H. B., Eds.; Addison-Wesley: Reading, MA, 1982; Part II, pp 89-152. (c) Li, X. Y.; Czernuszewicz, R. S.; Kincaid, J. R.; Spiro, T. G. *J. Am. Chem. Soc.* **1989**, *111*, 7012-7023.
(5) Argade, P.; Sassaroli, M.; Rousseau, D. L.; Inubushi, T.; Ikeda-Saito, M.; Lapidot, A. *J. Am. Chem. Soc.* **1984**, *106*, 6593-6596.
(6) Nagai, K.; Kitagawa, T.; Morimoto, H. *J. Mol. Biol.* **1980**, *136*, 271-289.
(7) Hori, H.; Kitagawa, T. *J. Am. Chem. Soc.* **1980**, *102*, 3608-3613.
(8) (a) Desbois, A.; Lutz, M.; Banerjee, R. *Biochemistry* **1979**, *18*, 1510-1518. (b) Kitagawa, T. In *Biological Applications of Raman Spectroscopy*; Spiro, T. G., Ed.; Wiley: New York, 1988; Vol. 3, pp 97-131.
(9) Springer, B. A.; Sligar, S. G. *Proc. Natl. Acad. Sci. U.S.A.* **1987**, *84*, 8961-8965.
(10) Morikis, D. Ph.D. Thesis, Department of Physics, Northeastern University, 1990.
(11) Egeberg, K.; Springer, B.; Martinis, S.; Sligar, S. G.; Morikis, D.; Champion, P. M. *Biochemistry* **1990**, *29*, 9783-9791.

0002-7863/91/1513-9655$02.50/0

of ^{15}N incorporation was determined to be >93% using the Rittenberg technique.[12] In addition, ^{15}N NMR results identified the presence of ^{15}N-labeled histidine amide and N_ϵ nitrogens.[13] This ^{15}N-labeled myoglobin was then reconstituted with ^{14}N heme.[14] The native sperm whale myoglobin was obtained from Sigma Chemical Co. in lyophilized form. The samples were prepared in pH 6 potassium phosphate buffer and were approximately 70 μM in protein. The native material obtained from Sigma was centrifuged to eliminate precipitates. Absorption spectra of all samples were taken to insure the sample integrity before and after resonance Raman experiments were performed. DeoxyMb was made by chemical reduction of metMb using aqueous sodium dithionite in a sealed deoxygenated sample cell. MbCO samples were prepared by flushing deoxygenated metMb samples with CO gas before addition of sodium dithionite.

Sample preparation and experimental conditions for the His(F8)Tyr Mb mutants and associated wild-type samples are described elsewhere,[10,11] and those for the pH studies of MbCO are given in Sage et al.[15] Human metHb samples were obtained in lyophilized form from Sigma and concentrated stock solution was centrifuged to eliminate precipitates. Purified human HbO_2 in potassium phosphate buffer was kindly provided by Professor M. J. McDonald. HbCO was made by flushing HbO_2 solution with CO gas for several minutes. Sample concentrations were approximately 100 μM in protein. All HbCO and HbO_2 data were taken with samples in spinning cells and incident laser powers of 5–10 mW to minimize photolysis. All other experimental conditions were similar to those of the labeling experiments described above.

Native and ^{15}N-labeled samples were prepared simultaneously, and data were collected using a SPEX Triplemate triple monochromator and a Princeton Instruments IRY1024 optical multichannel analyzer (OMA). Native and ^{15}N-labeled samples were run back-to-back without moving the monochromator grating between samples. The laser source was a Coherent CR-599 tunable CW dye laser with Stilbene III dye, pumped by a Coherent Innova 100 Ar ion laser. The laser power at the sample was typically 10 mW after being filtered by a premonochromator. The excitation wavelengths were 416 nm for metMb, 430 nm for deoxyMb, and 420 nm for MbCO, near the Soret maxima for each species. The MbCO samples were run in a cylindrical spinning cell with incident power ~5 mW to minimize photolysis. Exposure times were typically 10 min for all samples.

All Raman spectra are frequency calibrated using neat fenchone and span the frequency range 100–900 cm^{-1} with a resolution of about 1.2 diodes per cm^{-1}. The sample spectra are flat-field corrected, which entails dividing the sample spectrum by a long-exposure white light spectrum to eliminate the fixed pattern noise due to the diode-to-diode detector response variations.

For the labeling data, linear backgrounds are subtracted from both the native and corresponding labeled spectrum in order to set the base line of the spectra to zero. The spectra of a native/labeled pair are normalized to approximately equal intensities, in order to correct for slight differences in protein concentration, incident photon flux, integration times, and scattered light alignments. More accurate normalization can be achieved on a peak-by-peak basis by using slightly different linear backgrounds and normalization constants for each pair of peaks in the native and labeled spectra. The labeled spectra are subtracted from the corresponding native spectra to obtain the difference spectra shown in the figures.

The experimental wavenumber shift of a mode in the labeled spectrum relative to the corresponding native spectrum is denoted by Δ. Positive Δ values correspond to a downshift in the labeled spectrum. Experimental Δ values are calculated from the differential intensities of the particular mode in the difference spectrum using the following equation[16]

$$\Delta = 0.38\Gamma\frac{I_D^0}{I^0} \qquad (1)$$

where Γ is the FWHM of a least-squares Lorentzian fit to the peak, I^0 is the scattering intensity at the peak, and I_D^0 is the maximum minus the minimum intensity in the difference spectrum for the shifted mode.

We have found that the back-to-back spectra sometimes show systematic frequency shifts Δ of order ± 0.2 cm^{-1} in the ν_7 skeletal mode, which is not expected to show any isotopic shift with $^{15}N_{His}$. This might be due to slight changes in the position of the laser line or thermal effects on the grating position during data collection. In these cases, the ν_7 mode is used as a reference frequency to correct for these systematic instrumental frequency shifts. All spectra contain the ν_7 mode as well as the lower frequency modes of interest. Thus, the small $\Delta\nu_7$ values for the ν_7 modes are subtracted from those of the other modes to obtain a corrected net isotopic shift Δ^n. The experimental uncertainties in the Δ values are estimated by equating I_D^0 in eq 1 to the RMS width of the scatter in the difference spectrum in the region of the particular peak.

Theoretical isotopic shifts Δ^{Fe-N} and Δ^{Fe-Im} are calculated using a simple two-body model which assumes either a Fe–N or a Fe–His oscillator. The masses used are 14 amu for nitrogen and 67 amu for the histidine imidazole ring in the native sample and 15 amu and 69 amu for the labeled masses, respectively. In addition, we have considered the possibility that the Fe and N_ϵ move together as a unit against the remaining mass of the imidazole, and we denote this calculated shift by $\Delta^{Fe-Im'}$. The masses used in this calculation are 70 amu for the Fe + N_ϵ mass and 53 amu for the remaining imidazole ring mass. The calculated quantities are given by

$$\Delta^{calc} = \bar{\nu}\left(1 - \sqrt{\frac{\mu}{\mu^*}}\right) \qquad (2)$$

where $\bar{\nu}$ is the experimental Raman frequency of the unlabeled sample, and μ and μ^* are the reduced masses $\mu = m_1m_2/(m_1 + m_2)$ of the native and labeled species, respectively.

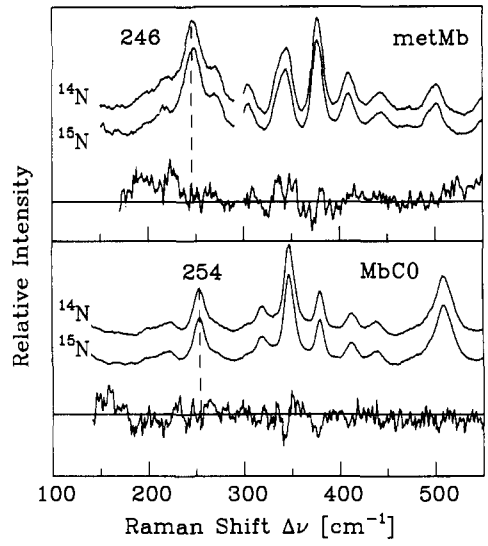

Figure 1. Resonance Raman and difference spectra of metMb (top panel) and MbCO (bottom panel). The bottom curve in each panel is the native minus the labeled difference spectrum. Excitation wavelengths are 416 nm for metMb and 420 nm for MbCO. The solid horizontal lines are the zeros of differential intensity for the difference spectra. The vertical scales of the difference spectra are expanded relative to the Raman data by factors of 10 (metMb) and 12 (MbCO). The regions 100–290 and 295–600 cm^{-1} of metMb have been analyzed independently as discussed in the text. No isotopic shift > 0.2 cm^{-1} is observed in the metMb 246-cm^{-1} mode or the MbCO 254-cm^{-1} mode.

Table 1.[a] Observed Isotopic Shifts

mode	Δ	$\Delta\nu_7$	net shift, Δ^n	mean, Δ^n
metMb, 246 cm^{-1}	0.0 ± 0.2	0.0 ± 0.1	0.0 ± 0.2	0.0 ± 0.2
	0.6 ± 0.2	0.6 ± 0.1	0.0 ± 0.2	
deoxyMb, 150 cm^{-1}	0.0 ± 0.8	0.2 ± 0.1	−0.2 ± 0.8	−0.1 ± 0.9
	0 ± 1	0.0 ± 0.1	0 ± 1	
deoxyMb, 218 cm^{-1}	1.3 ± 0.2	0.2 ± 0.1	1.1 ± 0.2	1.25 ± 0.2
	1.4 ± 0.2	0.0 ± 0.1	1.4 ± 0.2	
MbCO, 254 cm^{-1}	0.0 ± 0.2	−0.1 ± 0.1	0.1 ± 0.2	0.0 ± 0.2
	0.2 ± 0.2	0.2 ± 0.1	0.0 ± 0.2	

[a] All units cm^{-1}. Results of two independent measurements for each mode. Here Δ is the shift in cm^{-1} calculated by subtracting the $^{15}N_{His}$ isotopically labeled sample from the native sample. The net shift for the data of this work is calculated by using $\Delta\nu_7$ as an internal reference.

(12) Mulvaney, R. L.; Fohinger, C. L.; Bojan, V. J.; Michlik, M. M.; Herzog, L. F. *Rev. Sci. Instrum.* **1990**, *61*, 897–903.
(13) Theriault., Y.; Wright, P.; Chiu, M.; Sligar, S. Unpublished results.
(14) Teale, F. W. J. *Biochim. Biophys. Acta* **1959**, *35*, 543–549.
(15) (a) Sage, J. T.; Morikis, D.; Champion, P. M. *Biochemistry* **1991**, *30*, 1227–1236. (b) Sage, J. T.; Li, P.; Champion, P. M. *Biochemistry* **1991**, *30*, 1237–1247.
(16) Rousseau, D. L. *J. Raman Spectrosc.* **1981**, *10*, 94–99.

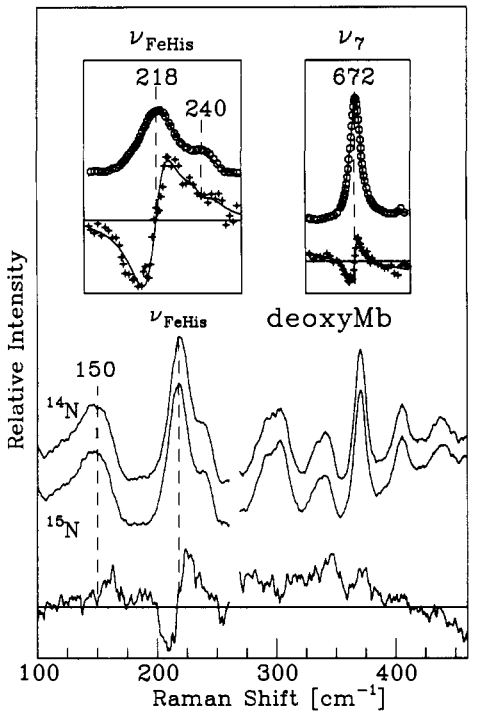

Figure 2. Resonance Raman spectra and difference spectra are shown for the low-frequency modes of deoxyMb along with an expanded plot of the ν_{FeHis} region (left insert) and the ν_7 region (right insert). Excitation wavelength is 430 nm. The top pair of curves in the main panel are the native (^{14}N) and ^{15}N-labeled globin samples, and the bottom curve is the difference spectrum. The regions 100–260 and 260–460 cm^{-1} have been analyzed independently. The inserts show the native spectrum (circles) with its Lorentzian fit (solid line). The crosses shown in the inserts are the difference spectra, and the solid lines passing through them are the difference curves of the native minus labeled Lorentzian fits. The horizontal lines are the zeros of differential intensity. In the deoxyMb species, an average isotopic shift of 1.25 cm^{-1} is seen for the 218-cm^{-1} mode. The shift in the ν_7 band corresponds to a 0.2-cm^{-1} instrumental shift, which is subtracted from that of the 218-cm^{-1} band, as described in the text. The vertical axes of the difference spectra are expanded by a factor of 10 relative to the Raman spectra.

Results

Isotopic-Labeling Experiments. Figure 1 shows the results of the ^{15}N-labeling experiments on metMb and MbCO. The top curve in each panel is the native Raman spectrum, the second is the labeled spectrum, and the third curve is the difference spectrum of the native spectrum minus the isotopically labeled spectrum. The resulting net isotopic shifts, calculated as described above, are reported in Table I. Figure 2 shows the deoxyMb spectra along with two inserts which show expanded plots of the 218-cm^{-1} and ν_7 modes. In the inserts, the circles are the unlabeled data and the crosses are the difference data. The solid lines are Lorentzian fits to the unlabeled Raman line shapes from which are subtracted similar fits to the labeled lineshapes to give the solid curves passing through the difference spectra.

The 246-cm^{-1} mode of metMb (top panel of Figure 1) and the 254-cm^{-1} mode of MbCO (bottom panel of Figure 1) show no shift greater than ±0.20 cm^{-1}. No other modes in the low-frequency region of metMb and MbCO display an isotopic shift outside experimental error. The small features in the difference spectra between 300 and 400 cm^{-1} are a result of the systematic error discussed above and of imperfect normalization of the peak intensities. We also found that the 254-cm^{-1} mode of MbO_2 does not show any isotopic shift upon labeling of the globin nitrogens (data not shown). Walters and Spiro[17] reported a 3-cm^{-1} shift in the 272-cm^{-1} mode of MbO_2 upon $^{18}O_2$ labeling and attributed this band to the ν_{Fe-His} mode. Our results show no significant isotopic shift (<0.2 cm^{-1}) of the 272-cm^{-1} band upon $^{15}N_{His}$ labeling. In addition, we observed no isotopic shift (0 ± 0.2 cm^{-1}) in the metMb 246-cm^{-1} mode with simultaneous $^{15}N_p$ and $^{15}N_{His}$ labeling.

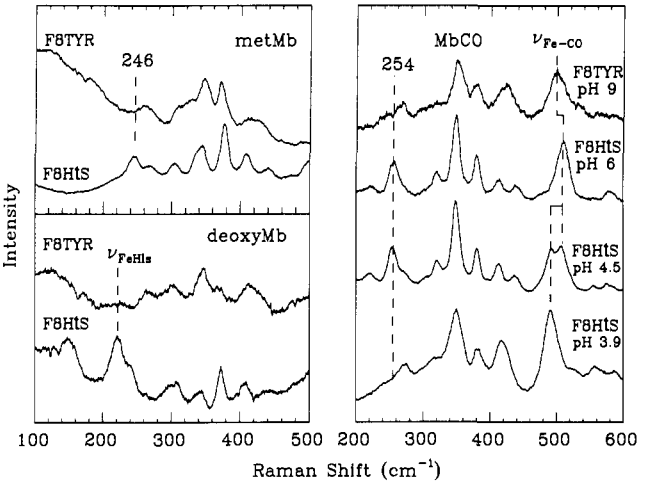

Figure 3. Low-frequency resonance Raman spectra comparing the effect of the mutation of the F8 proximal histidine (F8**HIS**, native Mb) to tyrosine (F8TYR) in metMb, deoxyMb, and MbCO. Also shown is the effect of low pH on the low-frequency spectrum of MbCO. Note that the 246-cm^{-1} mode of native metMb, the 218-cm^{-1} mode of native deoxyMb, and the 254-cm^{-1} mode of native MbCO disappear from the corresponding F8TYR mutant spectra. The lower three spectra of the right-hand panel show native MbCO at pH 6, 4.5, and 3.9. Note the disappearance of the 254-cm^{-1} mode at the lowest pH associated with the partial unfolding of the globin. Excitation frequencies for the various species are the same as Figures 1 and 2.

As can be seen from Table I, the deoxyMb mode at 218 cm^{-1} shows an average downshift, Δ^n = 1.25 cm^{-1}, when the globin is labeled with ^{15}N, consistent with a ν_{Fe-His} assignment.[2,5] There appear to be no isotopic shifts of the 150- or 240-cm^{-1} modes of deoxyMb outside the experimental errors.

Studies of Mb Mutants. Site-directed mutant studies of Mb His(F8)Tyr have shown that when the proximal F8 histidine is replaced by tyrosine, the 246-cm^{-1} mode of metMb and the 254-cm^{-1} mode of MbCO disappear (see Figure 3).[10,11] This might be taken as evidence for a Fe–His assignment for the 246- and 254-cm^{-1} modes, since they disappear when the Fe–His bond is replaced. However, since the $^{15}N_{His}$-labeling studies show no isotopic shifts for these modes, they cannot be associated with any modes involving motion of the N_ϵ of the His(F8).

Figure 3 also shows that the 150-, 218-, and 240-cm^{-1} modes of deoxyMb disappear in the His(F8)Tyr mutant with no new modes appearing in this region. The disappearance of the 218-cm^{-1} mode is consistent with a Fe–His mode assignment, but it is difficult to explain the disappearance of the 150- and 240-cm^{-1} modes since there are no isotopic shifts associated with these modes. Assignments for the 150- and 240-cm^{-1} modes will be discussed below.

The bottom three spectra in the right-hand panel of Figure 3 show MbCO at pH 6, 4.5, and 3.9. The 254-cm^{-1} mode is present at pH 6 and 4.5 but vanishes completely below pH 4, where the spectrum strongly resembles that of the His(F8)Tyr mutant. The disappearance of the 254-cm^{-1} mode below pH 4 corresponds to a partial unfolding of the globin.[15a] However, the appearance of the 218-cm^{-1} mode in the 10-ns transient Raman spectrum using a spinning cell indicates that the Fe–His bond remains intact in MbCO below pH 4.[15b] This suggests that a particular histidine–heme structural arrangement, which is only present in the fully folded structure of Mb, is responsible for the activity of the 254-cm^{-1} mode. Note that the 254-cm^{-1} mode is still present at pH 4.5 where the doublet in the Fe–CO stretching region corresponds to roughly equal populations of the "open" (ν_{Fe-CO} = 490 cm^{-1}) and "closed" (ν_{Fe-CO} = 508 cm^{-1}) states.[18]

(17) Walters, M. A.; Spiro, T. G. *Biochemistry* **1982**, *21*, 6989–6995.

(18) Morikis, D.; Champion, P. M.; Springer, B. A.; Sligar, S. G. *Biochemistry* **1989**, *28*, 4791–4800.

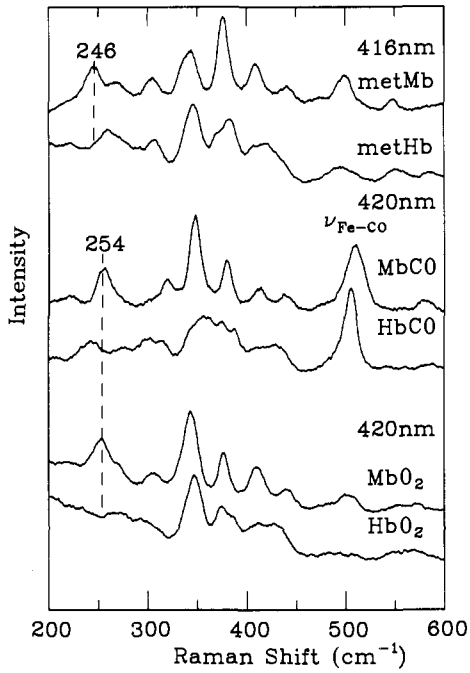

Figure 4. Low-frequency resonance Raman spectra of metMb and metHb (top pair), MbCO and HbCO (middle pair), and MbO_2 and HbO_2 (bottom pair). All pH values are 7. Excitation wavelengths are 416 nm for the met samples and 420 nm for the CO- and O_2-bound samples. Note the absence of the 246-cm^{-1} band of native metMb from the spectrum of native metHb and the absence of the 254-cm^{-1} band of native MbCO and native MbO_2 from the HbCO and HbO_2 spectra.

Low-Frequency Mb and Hb Comparisons. Figure 4 shows the low-frequency spectra of metMb, CO-bound, and O_2-bound monomeric Mb and the corresponding tetrameric Hb species. The 246-cm^{-1} mode of metMb is clearly absent from the metHb spectrum, and other less dramatic differences between the spectra can be observed. The 254-cm^{-1} modes of MbCO and MbO_2 are also distinctly absent from the corresponding Hb spectra. These differences are in contrast to deoxyMb and deoxyHb (data not shown), which both exhibit the Fe–His(F8) mode at ~218 cm^{-1}.

In summary, the His(F8)Tyr mutants of Mb lack the 246 cm^{-1} mode of metMb, the 150-, 218-, and 240-cm^{-1} modes of deoxyMb, and the 254-cm^{-1} mode of native MbCO. The 1.25-cm^{-1} isotopic shift of the 218-cm^{-1} band suggests its assignment as the Fe–His mode in deoxyMb. However, the bands at ~250 cm^{-1} in metMb and MbCO do not exhibit $^{15}N_{His}$ isotopic shifts and cannot be assigned to the Fe–His mode. These bands are not observed in the corresponding Hb species or in the partially unfolded state of MbCO at pH < 4. Possible assignments for these modes and their unique behavior will be discussed below.

Discussion

Low-Frequency Modes of DeoxyMb. The distinct isotopic shift of the 218-cm^{-1} mode in the $^{15}N_{His}$-labeled Mb and its disappearance in the Raman spectrum of the His(F8)Tyr mutant confirm[2,5] that it involves His(F8) motion. The magnitude of the isotopic shift (1.25 ± 0.2 cm^{-1}) agrees well with the calculated shift on the basis that the entire His(F8) imidazole ring is involved in a Fe–His vibration (Δ^{Fe-Im} = 1.4 cm^{-1}, Table II). In contrast, Argade et al. found a 1.7-cm^{-1} isotopic shift in the 218-cm^{-1} mode between ^{54}Fe- and ^{57}Fe-labeled Mb,[5] which is much smaller than predicted using the full imidazole ring mass (Δ^{Fe-Im} = 3.2 cm^{-1}), but similar to the result calculated using a single nitrogen mass (Δ^{Fe-N} = 1.2 cm^{-1}, Table II). Argade et al. attributed the small value of the Fe isotopic shift to mixing of the Fe–His mode with either an internal mode of the His(F8) or with a porphyrin skeletal mode. They also found that $^{15}N_p$ substitution of the porphyrin nitrogens did not shift the 218-cm^{-1} mode. This indicates that the 218-cm^{-1} mode does not contain a significant contribution from any mode involving motion of the porphyrin nitrogens, such as pyrrole tilting modes.[4]

Table II.[a] Deoxy Mb 218-cm^{-1} Mode

isotopic substitution	observed shift	calculated shifts[b]			
		Δ^{Fe-N}	Δ^{Fe-Im}	Δ^{eff}	$\Delta^{FeN-Im'}$
$^{14}N_{His}$–$^{15}N_{His}$	1.25 ± 0.2	5.9	1.4	1.25	1.8
^{54}Fe–^{57}Fe	1.7[c]	1.2	3.2	1.7	2.0
^{1}H–^{2}D	1.4[c]	0	0.75	0.6	1.2
$^{14}N_p$–$^{15}N_p$	0[c,d]	0	0	2.2	0
$\Sigma\lvert\Delta^{obs} - \Delta^{calc}\rvert$		6.55	2.3	3.0	1.05

[a] All units cm^{-1}. [b] The Δ^{Fe-N} are two-body calculations assuming only the iron atom and N_ϵ are involved in the vibration; the Δ^{Fe-Im} are two-body calculations assuming the entire imidazole mass (67 amu) is involved in the vibration. The Δ^{eff} values are calculated using masses m_{Im}^{eff} = 88 amu and m_{heme}^{eff} = 92 amu, which are effective masses consistent with the magnitude of the ^{15}N globin labeling shift and the Fe isotopic shift (ref 5) of the 218 cm^{-1} band. The $\Delta^{FeN-Im'}$ values are calculated assuming that the Fe–N_ϵ moves as a unit against the rest of the imidazole mass, m_{FeN} = 70 amu, and $m_{Im'}$ = 53 amu. [c] Taken from ref 5. [d] However, Δ = 1.5 cm^{-1} for model compounds (ref 19).

Within the two-body model we can find the effective masses needed to be consistent with the $^{15}N_{His}$ and ^{57}Fe isotopic shifts. We find m_{Im}^{eff} = 88 ± 6 amu for the nitrogen-containing imidazole mass and m_{heme}^{eff} = 92 ± 6 amu for the iron-containing heme mass in order to reproduce the $^{15}N_{His}$ and ^{54}Fe shifts to within experimental error. The value for m_{heme}^{eff} is much larger than the iron atom mass, but close to the mass of the iron atom plus the four porphyrin nitrogens (112 amu). However, significant involvement of the porphyrin nitrogens in the 218-cm^{-1} mode cannot be reconciled with the absence of isotopic sensitivity[5] to $^{15}N_p$ substitution.[19] Thus, the large value found for the effective mass of iron must be viewed as evidence that additional nuclear motions, not involving the N_p, are mixed with the iron motion to form the 218-cm^{-1} mode.

The observed isotopic shift of the 218-cm^{-1} band due to ^{2}H labeling of Mb has been reported[5] to be 1.4 cm^{-1} (Table II), which is slightly larger than the magnitude of the isotopic shift observed for $^{15}N_{His}$ labeling (1.25 cm^{-1}). The larger isotopic shift in the ^{2}H studies is inconsistent with the oscillation of the entire imidazole mass against the iron atom, since there is a 2 amu change in the $^{15}N_{His}$ experiment and only a 1 amu change in the ^{2}H experiment (1 labile proton). As a result, we have explored another model which assumes that the motion involves the Fe and N_ϵ moving together against the rest of the imidazole ring mass. This model predicts the shifts, $\Delta^{FeN-Im'}$, given in Table II, and agrees well with the absence of a $^{15}N_p$ effect and with the observed magnitude of the deuterated isotopic shift and the Fe labeling experiments. The predicted magnitude of the $^{15}N_{His}$ isotopic shift, 1.8 cm^{-1}, is close enough to the observed value that this model deserves serious consideration. An alternative explanation[5] for the large isotopic shift observed in the ^{2}H experiment is that the deuteration of all labile protons in the globin may induce a protein structural change that slightly alters ν_{Fe-His}. However, even when the ^{2}H experiment is not considered, the calculated $\Delta^{FeN-Im'}$ shifts still yield the best agreement with the remaining data in Table II. Because the 218-cm^{-1} mode involves primarily Fe and His(F8) motion but may not be associated with a simple Fe–His stretch, we refer to it as ν_{FeHis} rather than ν_{Fe-His}. In fact, the 218-m^{-1} mode is probably more complex than this simplistic model would suggest, but it seems likely that internal motions of the histidine make a significant contribution. Ultimately, the isotopic shift data should

(19) Desbois, A.; Momenteau, M.; Loock, B.; Lutz, M. *Spectrosc. Lett.* **1981**, *14*, 257–269. In this work, it was reported that the modes at 205 cm^{-1} of the model compounds Fe(II)PP 2MeIm and Fe(II)etioP 2MeIm are N_p isotope sensitive, with Δ = 1.5 cm^{-1}. This observed magnitude is close to the calculated shift (1.6 cm^{-1}) assuming that all four N_p nitrogens are involved in the motion and that the entire 2-methylimidazole mass is used in the calculation. However, the reliability of this data has been questioned.[5] Additional measurements in this laboratory, involving simultaneous substitution of $^{15}N_p$ and $^{15}N_{His}$ in Mb show shifts Δ^n ~ 1.2 cm^{-1}, which are the same as when only $^{15}N_{His}$ is substituted. This supports the work of Argade et al.[5] and suggests that the N_p do not participate in the motions associated with the 218-cm^{-1} mode.

be used in constructing a complete normal mode description of the heme–histidine system. The correct prediction of the various isotopic shifts is a stringent experimental test that must be applied in such an analysis.

The 150-cm^{-1} mode of deoxyMb (Figure 2) is a depolarized doublet with a blue-shifted REP.[20] Ondrias et al. have speculated that the 150-cm^{-1} mode may be associated with a radically different conformation of the Fe–His bond.[21] This suggestion is inconsistent with the absence of an isotopic shift in the $^{15}N_{His}$ labeling experiments. However, since the experimental error in the shift of this mode is relatively large (Table I), the suggestion of Ondrias et al. cannot be entirely excluded. On the other hand, recent molecular dynamics calculations by Petrich et al. predict an oscillation with a time scale of ~200 fs (at 170 cm^{-1}) associated with torsional motion of the His(F8) plane about the heme normal.[22] Association of the 150-cm^{-1} mode with this type of motion would be consistent with the absence of a large (> 1 cm^{-1}) isotopic shift as well as with the disappearance of the 150-cm^{-1} mode in the His(F8)Tyr mutant.[10,11] The enhancement of such a mode in resonance with the Soret π–π^* transition could be due to a shift along the associated normal coordinate in the electronic excited state, caused by interaction of the imidazole with the π^* electron density on the porphyrin nitrogen. Since the π^* electron density on the porphyrin nitrogens is predicted to be quite different for the two quasi-degenerate excited states,[23] this enhancement mechanism would lead to highly asymmetric coupling to the x and y components of the Soret band. Such asymmetric coupling is expected to produce depolarization of the Raman scattering,[24] as observed for the 150-cm^{-1} mode.[20] In addition, it is conceivable that the interaction with the π^* orbital could blue-shift the coupled electronic transition sufficiently to account for the observed[20] REP of the 150-cm^{-1} mode. The orientation of the His(F8) may also be involved in the inhomogeneous broadening of the Soret band[25] through similar interactions.

Argade et al. found[5] a 1.5-cm^{-1} isotopic shift in the deoxyMb mode at 240-cm^{-1} when the porphyrin nitrogens were labeled with $^{15}N_p$, but we observe no isotopic shift within experimental error upon $^{15}N_{His}$ labeling of the globin. These facts along with the disappearance of the mode in the His(F8)Tyr mutant[10,11] support the suggestion of Argade et al. that the 240-cm^{-1} mode is an out-of-plane pyrrole tilting mode. This mode evidently becomes Raman active due to N_p–His(F8) interactions that break the porphyrin reflection symmetry.[4a]

Low-Frequency Modes of MetMb and MbCO. The site-directed mutant studies have shown that the modes at ~250 cm^{-1} are absent from the His(F8)Tyr mutants in the metMb and MbCO forms.[10,11] Thus, a *necessary* condition for the enhancement of these modes is the presence of Fe–His(F8) ligation. However, Fe–His(F8) ligation is not *sufficient* for the presence of the 250-cm^{-1} modes since there are cases in which the Fe–His(F8) bond is intact but the 250-cm^{-1} mode is absent. Examples include MbCO below pH 4, metHb, HbCO, and HbO_2 (see Figures 3 and 4). As we have seen, the modes at ~250 cm^{-1} in native metMb and MbCO show no detectable isotopic shifts (Figure 1), and therefore, they are not ν_{FeHis} modes involving motion of the N_ϵ. However, Teraoka and Kitagawa reported that the 246-cm^{-1} mode of metMb is Fe isotope sensitive,[3] and Choi and Spiro also observed Fe isotopic sensitivity in the 251-cm^{-1} mode of metMbF^- as well as in the 255-cm^{-1} mode of the ferric model compound $[(ImH)_2Fe^{III}OEP]^+$.[4a,b] On the basis of the Fe isotopic sensitivity, this mode was assigned[4a,b] to an out-of-plane concerted pyrrole tilting mode which involves motion of the central Fe atom. Unexpectedly, we found that the 246-cm^{-1} mode of metMb does not exhibit an isotopic shift upon simultaneous labeling of $^{15}N_{His}$ and $^{15}N_p$. This observation contrasts with the large (~3 cm^{-1}) $^{15}N_p$ isotopic shifts observed[4c] for the pyrrole tilting modes of NiOEP and suggests that a pyrrole tilting mode assignment for the modes at ~250 cm^{-1} may be too simplistic. An important observation, which may help in the correct assignment of the ~250-cm^{-1} modes, is that they are enhanced only when the His(F8) is ligated to the Fe and then only for specific histidine–heme conformations particular to the fully folded conformation of metMb, MbCO, and MbO_2 and to certain model compounds which possess the 250-cm^{-1} mode, such as $[(ImH)_2Fe^{III}OEP]^+$.

The evidence presented here suggests that the ~250-cm^{-1} modes can be used as sensitive structural markers related to the position of the His(F8) moiety with respect to the heme. For example, the loss of the 254-cm^{-1} mode of MbCO at low pH (Figure 3) is likely due to an alteration in the His(F8)–heme geometry that is coupled to the partial unfolding that occurs below pH 4. Similarly, the absence of the ~250-cm^{-1} mode in the Hb spectra strongly suggests a difference between the heme–His(F8) geometry of Mb (pH 7) and Hb. In the Hb tetramer, structural rearrangement at the heme might be induced by subunit association. However, resonance Raman spectra of the isolated α and β subunits (kindly provided by Prof. M. J. McDonald) in the CO-bound and O_2-bound forms did not reveal the presence of the ~250-cm^{-1} modes.[26] Thus, the absence of modes at ~250 cm^{-1} in HbCO and HbO_2 cannot be related to structural changes induced by subunit association. Nevertheless, the modes at ~250 cm^{-1} seem to be good markers for a unique histidine–heme conformation present in the fully folded conformation of metMb, MbCO, and MbO_2.

In order to correlate the ~250-cm^{-1} mode with possible structural differences between Mb and **H**b, we have compared X-ray crystallographic parameters of Mb and Hb. One parameter we have considered is the Fe–mean heme plane distance[27] which is slightly longer in deoxy**H**b. However, the trend reverses in the ligand bound forms (especially aquometMb) and there appears to be a larger iron displacement in the Mb samples. Thus, we tentatively suggest that structural interactions (such as eclipse of the histidine plane with the N_p–N_p axis) lead to larger Fe–mean heme plane distances in the ligand-bound forms and favor the enhancement of the ~250-cm^{-1} modes in Mb. This is consistent with X-ray crystal studies[28] which show a smaller eclipse angle for Mb in both the ligand-bound and deoxy forms.

In summary, we have confirmed that the mode at 218 cm^{-1} in deoxyMb involves significant His(F8) motion by observing a 1.25-cm^{-1} downshift in the $^{15}N_{His}$-labeled sample. The magnitude of this shift along with that reported[5] for Fe isotopically labeled Mb is consistent with a two-body oscillator calculation involving the entire histidine residue ($m_{His} \approx 93$ amu) and the central core of the heme ($m_{Fe-N_p} \approx 112$ amu). However, the involvement of N_p atoms is inconsistent with the reported[5] absence of an isotopic shift in $^{15}N_p$-labeled Mb. An alternative model for the 218-cm^{-1} mode involves concerted motion of the Fe–N_ϵ mass against the remaining imidazole mass and is reasonably consistent with the entire body of experimental evidence. However, a full normal mode treatment of the heme–histidine system is clearly needed to quantitatively account for all of the observed isotopic shifts of the 218-cm^{-1} mode. The depolarization ratio and REP of the 150-cm^{-1} mode in deoxyMb, along with the isotopic labeling and the His(F8)Tyr mutant spectra, are consistent with an assignment to torsional motion of the His(F8) about the heme normal. The isotopic labeling and site-directed mutant data are consistent with the 240-cm^{-1} mode of deoxyMb, the 246-cm^{-1} mode of metMb, and the 254-cm^{-1} mode of MbCO being associated with modes

(20) Bangcharoenpaurpong, O.; Schomacker, K. T.; Champion, P. M. *J. Am. Chem. Soc.* **1984**, *106*, 5688–5698.
(21) Ondrias, M. R.; Rousseau, D. L.; Shelnutt, J. A.; Simon, S. R. *Biochemistry* **1982**, *21*, 3428–3437.
(22) Petrich, J. W.; Lambry, J. C.; Kuczera, K.; Karplus, M.; Poyart, C.; Martin, J. L. *Biochemistry* **1991**, *30*, 3975–3987.
(23) Gouterman, M. *J. Mol. Spectrosc.* **1961**, *6*, 138–163.
(24) Sage, J. T.; Morikis, D.; Champion, P. M. *J. Chem. Phys.* **1989**, *90*, 3015–3032.
(25) (a) Šrajer, V.; Shomacker, K. T.; Champion, P. M. *Phys. Rev. Lett.* **1986**, *57*, 1267–1270. (b) Šrajer, V.; Champion, P. M. *Biochemistry* **1991**, *30*, 7390.
(26) Wells, A. Unpublished results.
(27) (a) Perutz, M. F. In *The Molecular Basis of Blood Diseases*; Stamatoyannopoulos, N., Ed.; Saunders: Philadelphia, 1987; pp 127–178. (b) Dickerson, R. E.; Geis, I. *Hemoglobin: Structure, Function, Evolution, and Pathology*; Benjamin Cummings: Menlo Park, CA, 1983.
(28) Phillips, S. E. V. *J. Mol. Biol.* **1980**, *142*, 531–554.

that are enhanced by heme-His(F8) interactions. Moreover, because HbO_2, HbCO, and metHb lack the modes at ~250 cm^{-1} observed in the corresponding Mb species, their enhancement must be associated with differences in heme-histidine conformation between Mb and Hb. Similar arguments hold for the native and partially unfolded (low pH) forms of MbCO. We tentatively suggest that the intensity of the ~250-cm^{-1} mode is a probe of the eclipse angle between the histidine plane and the N_p-N_p axis.

Acknowledgment. We thank Prof. M. J. McDonald for kindly providing human HbO_2 and isolated α- and β-Hb subunit samples. This work was supported by grants from the NIH (AM-35090) and NSF (90-16860).

Registry No. Fe, 7439-89-6; His, 71-00-1; heme, 14875-96-8.

Communications to the Editor

Enantioselective Synthesis of (+)-3-Isorauniticine via a Catalytic Tandem "Palladium-Ene"/Carbonylation Reaction

Wolfgang Oppolzer,* Hugues Bienaymé, and Arielle Genevois-Borella

Département de Chimie Organique, Université de Genève CH-1211 Genève 4, Switzerland

Received July 24, 1991

The heteroyohimbine alkaloid 3-isorauniticine, isolated from *Corynanthe mayumbensis*, has been shown to possess constitution and relative configuration **1**.[1] We present here the first total synthesis of (+)-**1**,[2] thereby assigning its absolute configuration.[3]

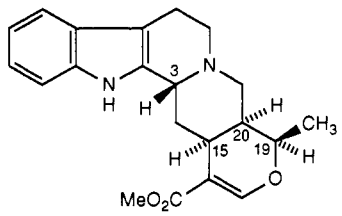

1

The cornerstone of our strategy is an intramolecular Pd-catalyzed allylation/carbonylation process, recently employed for a synthesis of (±)-pentalenolactone E.[4] For the preparation of **1** we envisaged control, in this key step, of the configuration of developing centers C(15) and C(20) by means of a preexisting center C(3).[5] To set up center C(3) we took advantage of a convenient multigram approach to enantiomerically pure α-amino acids (Scheme I).[6]

Thus, C-alkylation of commercially available chiral glycinate equivalent **2**[6,7] with allyl iodide/LiOH under phase-transfer conditions[6b] followed by acidic removal of the N-protecting group and N-acylation with mesitylenesulfonyl chloride provided crystalline sulfonamide **3**[8] (69% from **2**, mp 151-152 °C). N-Alkylation of **3** with (*Z*)-1-bromo-4-[(methoxycarbonyl)oxy]-2-butene[9] furnished dienylcarbonate **4** (96% yield).[8] Proceeding to the key reaction, carbonate **4** was subjected to Pd(0)-catalyzed cyclization/carbonylation in acetic acid, giving a 67:22:11 mixture of **5** and two stereoisomers.[10] Flash chromatography (FC) afforded the crystalline major isomer **5**[8] (mp 190-191 °C) in 45-53% yield.

Catalytic hydrogenation of **5** from the less hindered exo face and subsequent Baeyer-Villiger oxidation yielded lactone **6**[8] (mp 141-143 °C, 86% from **5**). We now needed to deprotect first the amino group and then the carboxyl group without affecting the lactone moiety. "Transesterification" of acyl sultam **6** with lithium *p*-nitrobenzyl oxide and FC gave the *p*-nitrobenzyl ester **7**[8] (55%, mp 118-119 °C). Starting from **7**, successive cleavage of the sulfonamide (HF/pyridine[11]), N-alkylation with tryptophyl bromide, and hydrogenolysis furnished carboxylic acid **8**[8] (62% from **7**), which was subjected to a $PhPOCl_2$-mediated Rapoport cyclization,[12] giving pentacyclic lactone **9**[8] (46%, mp 268-271 °C dec) as a single stereoisomer. The transformation **8** → **9** apparently involves decarbonylation of **8** with loss of the C(3) configuration, which is reestablished in the subsequent Pictet-Spengler step.

Finally, formylation of lactone **9** followed by Korte "rearrangement"[2a,c,g,j,13] provided (+)-3-isorauniticine (53% from **9**, hydrochloride: mp 258-260 °C dec, $[\alpha]_D$ = +37.4° (*c* = 0.77, MeOH, *T* = 19.5 °C); lit.[1] mp 277 °C, lit.[1] $[\alpha]_D$ = +25° (*c* = 1, MeOH)). The ^1H NMR, ^{13}C NMR, IR, and CD spectra of synthetic **1** are identical with those of the naturally occurring alkaloid.[14]

(1) Melchio, J.; Bouquet, A.; Païs, M.; Goutarel, R. *Tetrahedron Lett.* **1977**, 315-316.

(2) For syntheses of other, optically pure or racemic, heteroyohimbines, see: (a) Uskokovic, M. R.; Lewis, R. L.; Partridge, J. J.; Despreaux, C. W.; Pruess, D. L. *J. Am. Chem. Soc.* **1979**, *101*, 6742-6744. (b) Massiot, G.; Mulamba, T. *J. Chem. Soc., Chem. Commun.* **1984**, 715-716. (c) Hatakeyama, S.; Saijo, K.; Takano, S. *Tetrahedron Lett.* **1985**, *26*, 865-868. (d) Takano, S.; Satoh, S.; Ogasawara, K. *J. Chem. Soc., Chem. Commun.* **1988**, 59-60. (e) Hirai, Y.; Terada, T.; Yamazaki, T. *J. Am. Chem. Soc.* **1988**, *110*, 958-960. (f) Baggiolini, E. G.; Pizzolato, G.; Uskokovic, M. R. *Tetrahedron* **1988**, *44*, 3203-3208. (g) Hölscher, P.; Knölker, H.-J.; Winterfeldt, E. *Tetrahedron Lett.* **1990**, *31*, 2705-2706. (h) Hanessian, S.; Faucher, A.-M. *J. Org. Chem.* **1991**, *56*, 2947-2949. (i) Winterfeldt, E.; Radunz, H.; Korth, T. *Chem. Ber.* **1968**, *101*, 3172-3184. (j) Winterfeldt, E.; Gaskell, A. J.; Korth, T.; Radunz, H.-E.; Walkowiak, M. *Chem. Ber.* **1969**, *102*, 3558-3572. (k) van Tamelen, E. E.; Placeway, C.; Schiemenz, G. P.; Wright, I. G. *J. Am. Chem. Soc.* **1969**, *91*, 7359-7371. (l) Gutzwiller, J.; Pizzolato, G.; Uskokovic, M. R. *Helv. Chim. Acta* **1981**, *64*, 1663-1671; *J. Am. Chem. Soc.* **1971**, *93*, 5907-5908. (m) Wenkert, E.; Chang, C.-J.; Chawla, H. P. S.; Cochran, D. W.; Hagaman, E. W.; King, J. C.; Orito, K. *J. Am. Chem. Soc.* **1976**, *98*, 3645-3655. (n) Lounasmaa, M.; Jokela, R. *Tetrahedron Lett.* **1986**, *27*, 2043-2044. (o) Naito, T.; Kojima, N.; Miyata, O.; Ninomiya, I.; Inoue, M.; Doi, M. *J. Chem. Soc., Perkin Trans. 1* **1990**, 1271-1280.

(3) All heteroyohimbines were postulated to have the C(15) configuration as depicted in **1**. For the partial conversion (4%) of hirsuteine to 3-isorauniticine, see: Sakai, S.-I.; Shinma, N. *Chem. Pharm. Bull.* **1978**, *26*, 2596-2598.

(4) Oppolzer, W.; Xu, J.-Z.; Stone, C. *Helv. Chim. Acta* **1991**, *74*, 465-468.

(5) For the topological influence of preexisting centers on "palladium-ene" cyclizations, see: Oppolzer, W.; Keller, T. H.; Kuo, D. L.; Pachinger, W. *Tetrahedron Lett.* **1990**, *31*, 1265-1268.

(6) (a) Oppolzer, W.; Moretti, R.; Thomi, S. *Tetrahedron Lett.* **1989**, *30*, 6009-6010. (b) Oppolzer, W.; Zhou, C.; Moretti, R., publication in preparation.

(7) Oxford Chirality, PO Box 412, Oxford OX1 3QW, England.

(8) All new compounds were characterized by IR, ^1H NMR, ^{13}C NMR, and mass spectra.

(9) Obtained by successive treatment of (*Z*)-2-butene-1,4-diol with methyl chloroformate/pyridine and CBr_4/PPh_3 (59%).

(10) For the formation of annulated methylene cyclopentanones by "palladium-ene" cyclizations, see: Yamamoto, K.; Terakado, M.; Murai, K.; Miyazawa, M.; Tsuji, J.; Takahashi, K.; Mikami, K. *Chem. Lett.* **1989**, 955-958. Oppolzer, W.; Keller, T. H.; Bedoya-Zurita, M.; Stone, C. *Tetrahedron Lett.* **1989**, *30*, 5883-5886.

(11) Yajima, H.; Takeyama, M.; Kanaki, J.; Nishimura, O.; Fujino, M. *Chem. Pharm. Bull.* **1978**, *26*, 3752-3757.

(12) Johansen, J. E.; Christie, B. D.; Rapoport, H. *J. Org. Chem.* **1981**, *46*, 4914-4920.

(13) Korte, F.; Büchel, K. H. *Angew. Chem.* **1959**, *71*, 709-722.

0002-7863/91/1513-9660$02.50/0